

1-D and 2-D model atmospheres: iron and lithium LTE abundances in the Sun

A.S. Gadun and Ya.V. Pavlenko

The Main Astronomical Observatory of Academy of Sciences of Ukraine, Goloseevo, 252650 Kiev-22, Ukraine

Received 25 January 1996 / Accepted 15 January 1997

Abstract. We discuss LTE abundance determinations of iron and lithium in the solar atmosphere using a grid of one-dimensional (1-D) and two-dimensional (2-D) model atmospheres. These models differ mainly in the convection treatment. We found that the influence of atmospheric inhomogeneities on the iron abundance comprises ~ 0.1 dex for weak Fe I lines with low excitation potentials, and does not exceed ~ 0.05 dex for weak Fe II lines. 2-D models show lower iron abundances for Fe I lines. On the other hand, lithium abundances obtained for 1-D homogeneous and 2-D inhomogeneous model atmospheres differ up to 0.1–0.2 dex. 2-D model atmospheres result in lower lithium abundances, in contradiction with the recent suggestion of Kurucz (1995).

Key words: Sun: abundances – Sun: photosphere – line: formation

1. Introduction

Photospheres and line forming regions in solar-like stellar atmospheres lay practically on the upper part of their convective envelopes. Here metals are mainly in the form of ions due to their low ionization potentials. For this reason, small changes of the temperature structure in the stellar atmospheres caused by atmospheric inhomogeneities may strongly affect the intensity of metal absorption lines. In general, sizes and contrasts of inhomogeneities in stellar atmospheres depend on gravity $\log g$, effective temperature T_{eff} , and metallicity μ . On the other hand, results of the convection modeling depend on the procedure used in the computations. Mixing length theory (MLT) has been widely used to compute the convective flux in 1-D model atmospheres, but this approach involves strong assumptions.

Nordlund (1984), Steffen & Gigas (1985), Gadun (1986), Steffen (1989), and Atroshchenko (1993) carried out multidimensional hydrodynamic computations of the solar convection and used these multidimensional model atmospheres for LTE

computations of line profiles. Later, Bruls & Rutten (1993) performed NLTE computations of Na D₁ and K I 769.9 nm lines using three-dimensional (3-D) models of Stein & Nordlund (1989). Extensive LTE computations for 42 Fe I and 32 Fe II lines were carried out by Gadun (1994; see also Atroshchenko & Gadun 1994: hereafter Paper I) for two sequences of 3-D models: cool "grey" model atmospheres of Gadun (1986) and hot non-grey model atmospheres of Atroshchenko (1993). He showed that the impact of the atmospheric inhomogeneities on the abundance determination is in the range 0.03–0.04 dex for both Fe I and Fe II lines. Furthermore, the specific nature of 3-D models leads to abundance differences up to 0.1 dex for Fe I lines between 3-D and one-dimensional (1-D) models.

Recently, Gadun (1995) developed a new algorithm for the numerical simulation of convection. In the frame of his approach the radiative transfer equation is solved directly in 97 frequency intervals using the earlier ODF tables of Kurucz (1979). This scheme was used to compute a set of two-dimensional (2-D) models of the solar atmosphere (Gadun 1995; Gadun & Vorob'yov 1995; Gadun & Pikalov 1996). On the other hand, several attempts have been made to modify the MLT approach, and, recently, Kurucz (1993) implemented *convective overshooting* (CoOv) in his ATLAS9 program.

The aim of this paper is to investigate the dependence, in LTE, of lithium and iron lines on different treatments of the solar convection. Iron lines are widely used in astrophysics, and the study of Li I lines becomes especially important due to its implications on stellar structure and evolution models and because it has been questioned by Kurucz (1995).

2. Model atmospheres

To minimize the effect of possible errors in oscillator strengths and damping constants, we studied the differential dependence of Li and Fe abundances on model atmospheres of the Sun computed with different convection treatments.

2.1. 2-D models

2-D model atmospheres were computed using a system of equations of radiation hydrodynamics describing a compressible,

radiatively coupled, gravitationally stratified medium (Gadun 1995):

$$\frac{\partial \rho}{\partial t} + \frac{\partial \rho v_j}{\partial x_j} = 0, \quad (1)$$

$$\frac{\partial \rho v_i}{\partial t} + \frac{\partial \rho v_i v_j}{\partial x_j} = -\frac{\partial P}{\partial x_i} - \frac{\partial R_{ij}}{\partial x_j} - \rho g \delta_{i3}, \quad (2)$$

$$\begin{aligned} \frac{\partial \rho E}{\partial t} + \frac{\partial \rho E v_j}{\partial x_j} = & -\frac{\partial P v_j}{\partial x_j} - \frac{\partial R_{ij} v_i}{\partial x_j} + \\ & + \rho q_D - Q_R - \rho g v_3, \end{aligned} \quad (3)$$

where $i, j = 1, 3$, $E = E_v + e$ is the total specific energy (equal to the sum of kinetic energy E_v and internal energy e), P is the total pressure, R_{ij} is the Reynolds stress tensor $R_{ij} = \overline{\rho v'_i v'_j}$:

$$R_{ij} \approx \frac{2}{3} \rho (q_t + \sigma e_{kk}) \delta_{ij} - 2 \rho \sigma e_{ij}, \quad (4)$$

e_{ij} is a velocity deformation tensor, q_t is the specific kinetic energy of small-scale (sub-grid) turbulence, and σ is a kinematic coefficient of turbulent viscosity. The turbulent viscosity was treated with a simple local gradient model of Smagorinsky (1963):

$$\sigma = \frac{2(C_\sigma \Delta)^2}{\sqrt{2}} (e_{ij} e_{ij})^{1/2}; \quad (5)$$

then $q_t = (\sigma / C_\sigma / \Delta)^2 / 2$. $q_D = C_E q_t^{3/2} / \Delta$ is a dissipation of the kinetic energy of averaged movement at sub-grid level. Δ is the spatial step, $C_E = 1.2$, and $C_\sigma = 0.2$. Q_R is a divergence of the radiative energy flux (value of radiative heating/cooling).

The system of equations was integrated using the conservative large particle method (Belozerkovskiy & Davidov 1982). Usually this method is used with schemes of the first order of accuracy in space and time. In this work the order of accuracy in an approach of convective terms depends on the smoothness of the solution and varied up to second order in regions with the smooth flow.

The radiative energy transfer was treated by a momentum method (a differential approach) with the variable Eddington factors and LTE. Within the frame of this approach the complete momentum relation may be written for a given value of the radiative heating/cooling ($Q_{R\nu}$) as:

$$\frac{\partial}{\partial x_j} \frac{1}{\alpha_\nu} \frac{\partial}{\partial x_j} \frac{f_{\nu jj} Q_{R\nu}}{\alpha_\nu} = 4\pi \frac{\partial}{\partial x_j} \frac{1}{\alpha_\nu} \frac{\partial}{\partial x_j} f_{\nu jj} B_\nu + Q_{R\nu}, \quad (6)$$

where B_ν is the monochromatic Planck function, and $f_{\nu jj}$ the variable Eddington factors. Then $Q_R = \sum Q_{R\nu} \omega_\nu$, where ω_ν are the weights. The boundary conditions were used in the form:

$$\frac{1}{4\pi} \frac{\partial}{\partial z} \frac{f_{\nu zz} Q_{R\nu}}{\alpha_\nu} = \frac{\partial}{\partial z} \left(f_{\nu zz} - \frac{1}{3} \right) B_\nu, \text{ for } \tau_\nu = \tau_{\nu \max} \quad (7)$$

and

$$\frac{\partial}{\partial z} \frac{f_{\nu zz} Q_{R\nu}}{\alpha_\nu} = -\alpha_\nu q_{\nu z}^0 + 4\pi \frac{\partial}{\partial z} f_{\nu zz} B_\nu, \text{ for } \tau_\nu = 0, \quad (8)$$

where $q_{\nu z}^0$ is the vertical component of radiative flux at the upper boundary. The final equation with its boundary conditions can be solved using a standard difference technique. In the optically deep layers the diffusion approximation was taken for finding Q_R . The detailed frequency dependence of the monochromatic continuum opacity as well as the radiation transfer in spectral lines were taken into account. The line opacities were considered using directly the earlier Kurucz's opacity distribution function (ODF, Kurucz 1979) for standard solar abundances without molecular lines. The system of equations and the numerical techniques were described in detail by Gadun (1995).

In this work we consider two kinds of 2-D model atmospheres:

a) Quasi-stationary time-dependent models which describe only a single scale of the solar granulation (single scale or "one granule" -OG- approach, Gadun 1995). Thermal convection is treated in these models as quasi-stationary, cellular, and laminar. Topology of flows is not changed during the modeling process. These models have low Reynolds numbers ($Re < 120$). Due to the large influence of numerical viscosity and the absence of non-stationary interaction with neighbouring granules, the secondary motions in the upper layers are non-active, and photospheric velocity fields are governed by overshooting convection. Using these models it is possible to estimate the impact of the inhomogeneities on the lithium and iron abundances in the idealized approach, when these inhomogeneities are caused by the laminar, stationary and plane convective flows.

The size of the model region of OG models was chosen as 1295×2030 km in horizontal and vertical direction with a spatial step of 35 km. The atmosphere region occupies about 900 km. Although the flow topology in these models is time-independent they are affected by oscillations, and to take them into account we carried out the line computations over a short sample of time-dependent models. To consider a dependence of the synthesized line profiles on the wave component, computations were carried out for 11 models with a temporal step of 30 s between them. We also used two models obtained by the average of all 11 OG models at equal levels of τ_5 and equal geometrical height (h). Here τ_5 is a monochromatic optical depth at 5000 Å. Such models are labelled as OGA models.

b) Non-stationary multiscale models (MS) with dynamic interaction of several granules in the model region. The model region size, 3930×2030 km, was sampled with the same spatial step as in OG models. These models treat convection as a non-stationary process. The Reynolds number is higher ($Re < 550$) than for OG models. There are several evolved granulation flows with the interaction between them in the model regions. In these models, secondary motions in the middle and upper photosphere are very active. They have a significant impact on the radiative-dynamic state of photospheric layers, and the structure of these layers can be described more properly.

We note that the flow topology and the radiative-dynamic situation in the photosphere layers are strongly time-dependent. To exclude selection effects, we performed the synthesis of spectral lines over the whole sample of time-dependent MS models. Af-

terwards we carried out the temporal averaging procedure over 529 models with 30 s step. This corresponds to the integration time of $\sim 4^h 24^m$. Basic results concerning MS model computations, parameters of 2-D granules, and $k - \omega$ power spectra for these models are given in Gadun & Vorob'yov (1995) and Gadun & Pikalov (1996). Lines were also computed for the "averaged MS" (MSA) models which were obtained by averaging all 529 MS models over equal optical depths (τ_5) and geometrical height (h) levels.

A few important points are noted:

- by definition, OG and MS models are self-consistent. They define both the temperature structure and the velocity field in the modeling region.

- In fact, OGA and MSA models are "1-D-like" models. Strictly speaking, they are not self-consistent. In such averaged models the thermodynamic quantities are not consistent with the relation of hydrostatic equilibrium and the equation of state. To solve this problem, in Paper I the authors computed a new 1-D model where the temperature gradient was taken from the averaged 3-D model, and P and ρ were found from the equations of state and hydrostatic equilibrium. In this paper we are interested in the study of the impact of inhomogeneities on the abundance determination, and we consider only averaged models. Of course, the information about the velocity field is absent in the averaged OGA and MSA models. To compute the line profiles for these models we should define micro- and macro-turbulent velocity field parameters. These parameters can be directly obtained from 2-D models by the filtering of velocities over large- and small-scale structures. But, in principle, each line has its own filtering parameters. For this reason, we decided to work with 1-D models in the frame of the classical spectral line analysis. Namely, we used for them the micro- and macroturbulent velocities similar to those which were found for 1-D classical solar model atmospheres to fit weak FeI and FeII lines (see Section 4.1).

2.2. 1-D models

We obtained iron and lithium abundances in the solar atmosphere using also several 1-D model atmospheres:

- semiempirical HOLMU model atmosphere (Holweger & Müller 1974),
- theoretical Kurucz (1993) model atmosphere computed with convective overshooting (K93),
- theoretical model atmosphere (PK79) computed by the code SAM92. This program is a modification of ATLAS9 (Kurucz 1993). Opacity was considered in the frame of the opacity sampling approach, and the subroutine XLINOPOS was taken from SAM71 (Pavlenko 1991). To compute the blocking effect due to the absorption by lines of atoms and ions we used the list of Kurucz (1992). The mixing length theory parameter used was $\alpha = H_p/H_l = 1.25$, and the SAM92 model atmosphere was computed *without convective overshooting*. The temperature structure of that model is similar to that present in the Kurucz (1979) solar model.

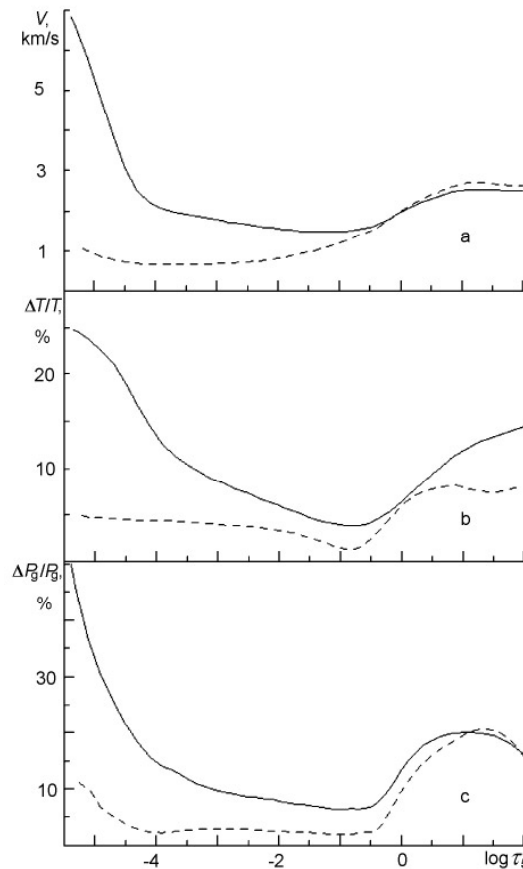


Fig. 1a–c. R.M.S. vertical velocities (a), fluctuations of the temperature (b), and gas pressure (c) at equal τ_5 levels in the sequences of MS and OG 2-D models. The data were obtained by averaging over the space and modeling time. Solid and dashed lines represent MS and OG models, respectively

2.3. Comparison of temperature structures of model atmospheres

R.M.S. vertical velocities and fluctuations of temperature and gas pressure in OG and MS models averaged over space and modeling time at equal τ_5 level are shown in the Fig. 1. The different behavior of the velocity field in OG and MS models, as well as the more pronounced fluctuations of thermodynamic values in MS models, may be explained by the presence of convective flows (inhomogeneities) of larger scales in these models and the interaction between them. The growth of the vertical velocity in the upper photosphere is the result of increasing oscillatory motions.

Temperature distributions in photospheric and in subphotospheric layers of 1-D models are shown in Fig. 2. We point out a few items:

- $T_{\text{HOLMU}} > T_{\text{K93}} > T_{\text{OGA}} > T_{\text{MSA}}$ and $T_{\text{MSA}} \approx T_{\text{PK79}}$ in the forming region of weak and intermediate Fe I lines with low excitation potential. The model K93 has higher temperatures in these layers in comparison with our 1-D models (PK79, OGA, and MSA) due to differences in opacity computation procedure and opacity source lists.

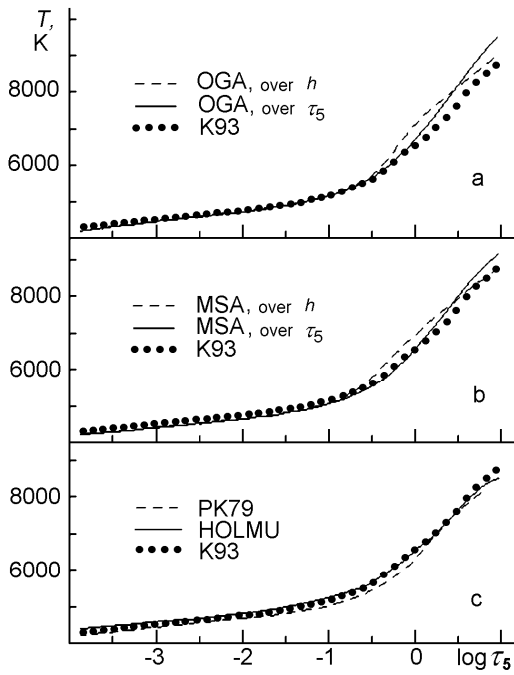


Fig. 2a–c. Temperature distributions in the models used: in atmospheric layers of OGA **a**, MSA **b**, and PK79 and HOLMU **c** models in comparison with 1-D hydrostatic models (K93) of Kurucz (1993)

- MSA and OGA models have the largest temperature gradients in the lower photosphere.
- Significant differences between averaged OG and MS models were found in the lower photosphere and in sub-photospheric layers. Their structures depend on the averaging procedure over equal τ_5 or h layers: models averaged over h are hotter near irradiating layers but they have cooler subphotospheric layers. Indeed, hot and cold structures in high temperature-dependent opacity regions provide different contributions due to the averaging procedure.
- The effect of the convective overshooting in the model K93 is obvious: temperatures in low photosphere become higher.

3. Line lists

The lists of weak Fe I and Fe II lines used are given in Tables 1 and 2, respectively. They were taken for a comparative analysis of iron abundance determination based on the chosen sets of 1-D and 2-D models. Central depths and equivalent widths of these lines observed in the solar spectrum were taken from Gurtovenko & Kostyk (1989: GK89). Note, the weak Fe I and Fe II lines were selected from Paper I, and were used there to obtain the iron abundance based on earlier 3-D models. Our Fe I lines have laboratory determined oscillator strengths by Blackwell et al. (1979, 1986). For the set of FeII lines we took the empirical oscillator strengths of Gurtovenko & Kostyk (1989) which are consistent with the Oxford system of oscillator strengths. For the Li I resonance doublet at λ 670.8 nm, we used data from Wiese et al. (1966).

Table 1. List of Fe I lines

λ , nm	E_{pl}	$\log(gf)$	W , pm	d
434.7242	0.00	-5.503	4.16	0.608
444.5479	0.09	-5.441	3.65	0.573
512.7688	0.05	-6.125	1.71	0.244
608.2718	2.22	-3.573	3.40	0.363
612.0249	0.91	-5.970	0.50	0.052
649.8945	0.96	-4.699	4.35	0.442
657.4254	0.99	-5.004	2.62	0.293
662.5025	1.01	-5.366	1.39	0.149
772.3210	2.28	-3.617	4.14	0.336
807.5158	0.91	-5.062	3.25	0.281

Table 2. List of Fe II lines

λ , nm	E_{pl}	$\log(gf)$	W , pm	d
408.7277	2.58	-4.68	1.36	0.176
463.5311	5.95	-1.59	1.88	0.211
467.0173	2.58	-4.21	3.12	0.355
500.0735	2.78	-4.70	1.02	0.115
510.0656	2.81	-4.33	1.92	0.210
513.2674	2.81	-4.16	2.55	0.271
513.6800	2.84	-4.45	1.48	0.158
541.4075	3.22	-3.77	2.66	0.290
608.4105	3.20	-3.96	2.10	0.203
611.3329	3.22	-4.26	1.20	0.111
636.9463	2.89	-4.28	2.01	0.172
751.5837	3.90	-3.60	1.44	0.112

To investigate how the 2-D HD models reproduce the profiles of spectral lines forming at different levels of the solar atmosphere, we analyzed the A_w and A_d behaviour, where abundances A_w and A_d were determined by the fit of equivalent widths and central intensities of absorption lines in the center of the Sun, respectively ¹. For this, we added a sample of stronger lines into Table 1 and Table 2. So, for OG models we used the whole list from Paper I containing 42 Fe I and 32 Fe II lines and for MS models A_w and A_d computations were performed for 17 Fe I and 18 Fe II lines only. In last case we used reduced set of lines from Paper I because A_w and A_d for MS models vary in dependence on line parameters not so strong as in the case of OG models. Preliminary results concerning the relative behavior of A_w and A_d of Fe I and Fe II lines for these 2-D models have been represented by Gadun (1996).

4. Line computations

Most of spectral line computations were performed with the code SPANSAT (Gadun & Sheminova 1988) in LTE. Equivalent width computations for Li I lines were carried out with the

¹ Throughout this paper abundances are given in the scale $\log N(\text{H}) = 12$

Table 3. Iron abundance from Fe I lines

N	λ , nm	HMUK93		PK790GA		OAMS		MSAOG		MS
		τ	h	τ	h	τ	h	τ	h	
1.	434.77.68	7.61	7.43	7.51	7.53	7.39	7.45	7.55	7.37	
2.	444.57.58	7.51	7.34	7.42	7.44	7.30	7.36	7.44	7.26	
3.	512.87.68	7.61	7.43	7.52	7.53	7.40	7.45	7.48	7.29	
4.	608.37.58	7.53	7.40	7.45	7.45	7.35	7.40	7.48	7.35	
5.	612.07.70	7.64	7.48	7.56	7.57	7.45	7.50	7.53	7.35	
6.	649.97.63	7.55	7.40	7.45	7.44	7.34	7.37	7.48	7.33	
7.	657.47.61	7.54	7.39	7.46	7.45	7.34	7.38	7.45	7.29	
8.	662.57.64	7.58	7.43	7.50	7.50	7.39	7.43	7.48	7.31	
9.	772.37.72	7.66	7.53	7.57	7.55	7.47	7.50	7.60	7.48	
10.	807.57.62	7.55	7.40	7.45	7.44	7.34	7.36	7.45	7.29	
A_w		7.64	7.58	7.42	7.49	7.49	7.38	7.42	7.49	7.33
σ		0.05	0.05	0.05	0.05	0.05	0.05	0.05	0.05	0.06

program WITA2 (Pavlenko et al. 1995). Van der Waals broadening with the correction factor $E = 1.5$ and Stark broadening were taken into account. It is interesting to note that the central intensities of spectral lines are more sensitive to NLTE effects (see GK89) than equivalent widths. For this reason, to study the impact of photospheric inhomogeneities on Li and Fe abundances we analyse A_w only.

4.1. 1-D, OGA, and MSA models

The motion field was treated in the frame of a height-independent microturbulent velocity (v_{mi}). All computations with 1-D models were performed with $v_{mi} = 1$ km/s. To fit the central intensity of the Li I line we also used a height-independent macroturbulent velocity $v_{ma} = 1.85$ km/s.

4.2. 2D models

Absorption lines of iron and lithium were computed for every vertical column of the model region. Afterwards the line profiles were averaged over space and modeling time as in Paper I.

5. Results

5.1. Iron

The abundance determination results (A_w) for our sample of Fe I and Fe II lines are given in Tables 3 and 4. The dependence of A_w and A_d on equivalent widths computed for OG and MS 2-D models is shown in Figs. 3 and 4.

5.1.1. Fe I and Fe II lines: A_w and A_d values obtained with 2-D models

From the modeling of Fe I lines we found (Fig. 3):

– qualitatively, the behavior of A_w and A_d for OG 2-D models is the same as that obtained in Paper I for 3-D models: there are systematic differences between A_w and A_d (for the 10 weak

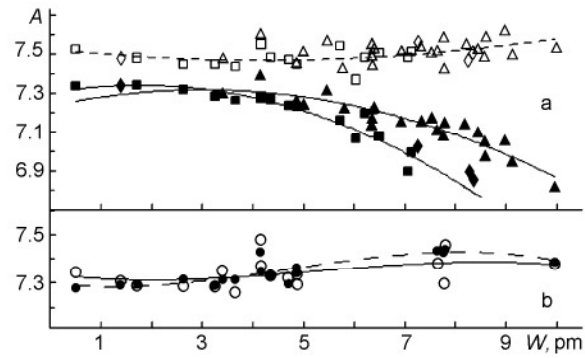


Fig. 3a and b. Iron abundances obtained from equivalent widths (open symbols) and central depths (filled symbols) for Fe I lines as a function of equivalent width. **a** OG 2-D models: squares correspond to lines with an excitation potential of 0–1 eV, diamonds – 1–2 eV, triangles – 2–3 eV. **b** Data from MS 2-D models.

lines given by Table 3 $\Delta = A_w - A_d \approx 0.18$ dex); A_d is strongly decreased for strong lines. As the main reason we may consider the deficit of a large-scale velocity field and NLTE effects (Paper I; Gadun 1996).

– The MS models have a statistically more extended spectrum of inhomogeneities. The absorption lines became less deep and wider. Note that A_d does not decrease even for strong lines. Moreover, the changes of A_w are weak too. As a result, the mean value of Δ strongly decreases down to ~ 0.01 dex for the 10 weak lines of Table 3.

For Fe II lines we found (Fig. 4):

– the behavior of A_w and A_d for OG 2-D models is qualitatively the same one as for Fe I lines: for the 12 weak lines of Table 4 we obtained $\Delta \approx 0.18$ dex, A_d values drop with the increase of line strength.

– as mentioned above, MS models have a statistically more extended spectrum of inhomogeneities and another temperature structure. As a result, the A_w values computed for MS are systematically slightly increased in comparison with OG models (Table 4). The behaviour of A_d changes strongly. For MS models, A_d values are increased. This effect depends on the line strength. For strong lines with $W > 8$ pm, A_d approaches to A_w – for the two strongest lines of our sample, the mean value of Δ is ≈ 0.02 dex. But for the 12 weaker lines of Table 4 Δ remains large: ~ 0.1 dex.

Comparing these and other results obtained for 3-D models (Gadun 1996), we note that:

1) in the case of the 3-D self-consistent models the problem of the sharp increase of Δ (due to the decrease of A_d) has not been solved (Paper I). The problem is solved by extending the statistical spectrum of inhomogeneities in the frame of 2-D MS models.

2) As Solanki & Steenbock (1988) showed, NLTE effects for low-excitation lines of Fe I may be ~ 0.1 dex for cool HSRA-like models. Low values of Δ , obtained for those lines with MS models in LTE may be a result of overestimation of the thermodynamic parameter and velocity field fluctuations in the

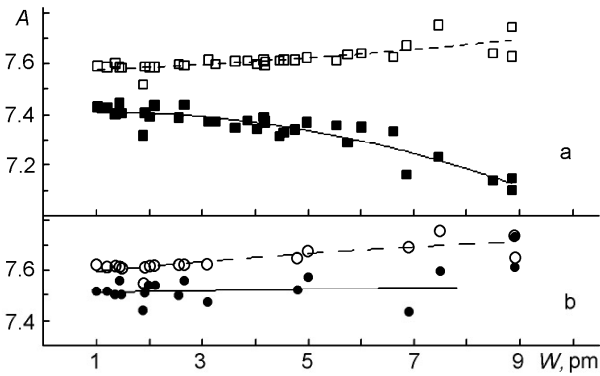


Fig. 4a and b. Iron abundances obtained from equivalent widths (open symbols) and central depths (filled symbols) for Fe II lines as a function of equivalent width. **a** OG 2-D models. **b** Data from MS 2-D models.

upper and middle model photosphere.

3) On the contrary, using lines of Fe II, we have obtained for 2-D MS models too large Δ for weak lines in comparison with the 3-D case (Paper I). This cannot be explained by NLTE effects, because these effects for Fe II lines are weaker by a factor of 10 with respect to Fe I lines. Possibly, these differences are caused by the details of the structure of 2-D models (see Gadun 1996 for details).

5.1.2. Fe I lines: A_w for set of 1-D models

We found that:

- the averaged abundance of iron obtained for 1-D models using Fe I lines shows a strong dependence on the temperature structure of models: $A_{\text{HOLMU}} > A_{\text{K93}} > A_{\text{OGA}} > A_{\text{PK79}} \approx A_{\text{MSA}}$. This result may be explained by the well known sensitivity of Fe I lines to the temperature structure of model atmospheres of solar-like stars.

- An impact of temperature inhomogeneities and velocity field on the iron abundance obtained for the Fe I lines is model-dependent. The A_w of Fe I lines formed in OG inhomogeneous model atmospheres are approximately equal to those corresponding to the averaged (OGA) ones (Table 3). But MS models show lower iron abundances in comparison with homogeneous MSA models. The difference increases up to 0.1 dex because MS models have a richer spectrum of inhomogeneities and a larger amplitude of their fluctuations (see Fig. 1) than OG models.

- The abundance of iron obtained for OGA models does not depend on the averaging procedure (over equal τ_5 or h level) of the models. This conclusion agrees well with that obtained previously for 3-D models (Paper I). However, in the case of MSA models we see a more pronounced difference between the results obtained for models averaged over τ_5 and h , because in the middle photosphere the differences in temperature structures of MSA models are more pronounced with respect to the OGA ones. We already mentioned above that in 2-D MS models there are convective flows of larger horizontal scales.

They can penetrate into higher photospheric layers in comparison with modest overshooting flows in 2-D OG models.

- As mentioned above, our "cool" 3-D models were computed in the frame of a rough model of the radiative transfer without taking into account the effective warming by spectral lines. Besides, "hot models" were obtained with overestimation of the effect of line warming. As a result, "hot" and "cool" 3-D models give too large and too small iron abundances for Fe I lines, respectively. Note that our new iron abundances obtained for Fe I lines differ strongly from those of 3-D models (Paper I).

5.1.3. Fe II lines: A_w for set of 1-D models

Fe II lines are less sensitive to the temperature structure of the solar-like atmospheres in comparison with Fe I lines (see, for example, GK89). For our grid of 1-D model atmospheres we obtained a similar result. However, we point out that iron abundances derived for 1-D models: HOLMU, K93, and PK79, differ from averaged 2-D models: OGA and MSA. Averaged 2-D models show lower iron abundances due to the higher temperature gradient in the lower photosphere. In our work we used oscillator strengths of Fe II lines computed by GK89 for the HOLMU model atmosphere and $A = 7.64$. Due to differences from the GK89 velocity field model and differences in computation procedure we have got a cloud of A_w values for our Fe II lines (Table 4).

The differences between 2-D and averaged models are less pronounced than for Fe I lines and are practically the same for both OG and MS model atmospheres. In the last case the differences do not exceed 0.05 dex.

The iron abundances obtained depend on the averaging procedure: for h -averaged models the abundances are higher. For OGA models this difference is not significant (~ 0.02 dex), and the effect is more evident for MSA (~ 0.05 dex).

Iron abundances obtained for 2-D models may be larger or smaller in comparison with values obtained for averaged models. The effect depends on the averaging procedure.

Iron abundance determined for 2-D models using Fe II lines agrees well with the value for 3-D models (Paper I), due to the low sensitivity of Fe II lines to temperature in solar-like atmospheres.

5.2. Lithium

We computed the strongest Li I resonance doublet line λ 670.776 nm in the spectrum of the solar disk center. Observations provide $d = 1 - I_{\lambda}^l/I_{\lambda}^c = 0.010$, $W_{\lambda} = 0.18$ pm (GK89).

5.2.1. 1-D models

In the frame of this work we studied the impact of the convective overshooting (Kurucz 1993) in 1-D model atmospheres on results of the lithium abundance determination. Two models with and without CoOv were computed with SAM92. We found that the lithium abundances A_w obtained for models with and without convective overshooting are 0.835 and 0.855, respectively.

Table 4. Iron abundance from Fe II lines

N	λ , nm	HMUK93	PK79	OGA	OGA	MS	MS	MS	MS
		τ	h	τ	h	τ	h	τ	h
1.	408.77.64	7.65	7.66	7.58	7.64	7.59	7.67	7.60	7.62
2.	463.57.64	7.65	7.71	7.50	7.56	7.55	7.62	7.52	7.55
3.	467.07.64	7.65	7.64	7.55	7.58	7.57	7.63	7.61	7.63
4.	500.17.64	7.66	7.65	7.57	7.61	7.59	7.65	7.59	7.62
5.	510.17.63	7.65	7.64	7.56	7.59	7.58	7.63	7.59	7.61
6.	513.37.64	7.66	7.64	7.56	7.58	7.58	7.63	7.60	7.60
7.	513.77.63	7.65	7.64	7.56	7.59	7.58	7.64	7.59	7.61
8.	541.47.64	7.66	7.65	7.55	7.57	7.58	7.62	7.59	7.59
9.	608.47.64	7.66	7.65	7.55	7.56	7.58	7.61	7.59	7.62
10.	611.37.64	7.66	7.66	7.57	7.58	7.59	7.63	7.59	7.61
11.	636.97.64	7.65	7.64	7.55	7.56	7.58	7.60	7.59	7.62
12.	751.67.65	7.67	7.67	7.56	7.56	7.60	7.61	7.59	7.62
A_w		7.64	7.66	7.65	7.56	7.58	7.58	7.63	7.59
σ		0.01	0.01	0.02	0.02	0.02	0.01	0.02	0.02

Table 5. Lithium abundances

Models	A_w	A_d	Δ
OG 2-D	0.89	0.84	0.05
OGA (τ)	0.95	0.91	0.04
OGA (h)	0.96	0.92	0.04
MS 2-D	0.74	0.67	0.07
MSA (τ)	0.84	0.80	0.04
MSA (h)	0.90	0.86	0.04

This means that the influence of CoOv on the Li abundance determinations in the solar atmosphere is rather weak.

5.2.2. 2-D models

Lithium abundances computed with 2-D and averaged models are given in Table 5. The value of Δ for 2-D inhomogeneous models is 0.05–0.07 dex, which lies between the values obtained for Fe I and Fe II lines.

The impact of inhomogeneities on the lithium abundance, which may be estimated as a difference between the lithium abundances obtained from 2-D models and from averaged ones,

is ~ 0.1 – 0.2 dex. We point out that these results are similar to those obtained for Fe I lines.

6. Discussion

Our computations were carried out for 2-D models of solar thermal convection. In the frame of our procedure, the radiative transfer was treated more explicitly than in an earlier paper (Atroschenko & Gadun 1994). This is important for the realistic modeling of the upper atmospheric layers. However, these 2-D models were obtained with the old ODF tables of Kurucz (1979). One may expect that a multidimensional simulation of the solar granulation with a larger list of atomic and molecular lines will give higher temperatures in the outer part of the atmosphere and higher values of iron and lithium abundances obtained from Fe I and Li I lines.

We have synthesized spectral lines without taking into account possible effects of horizontal radiative transfer. We expect that effects of multidimensional radiative transfer do not change our main conclusions (at least qualitatively), because a) we used weak lines, b) our main conclusions were based on the A_w analysis.

Our abundances were computed within the frame of LTE. The question arises whether NLTE may change our results. For lithium the answer is simple. Results of Steenbock & Holweger (1984), Pavlenko (1994), and Carlsson et al. (1994) show that NLTE effects for lithium lines are rather small in the solar atmosphere. NLTE lithium abundance corrections are less than ~ 0.05 dex. Moreover, lithium resonance lines are *photoionization controlled* (Thomas 1957). Indeed, NLTE lithium lines are less sensitive to the temperature structure of the outer atmospheric layers in comparison with LTE (Pavlenko 1995; Pavlenko et al. 1995). For iron lines the picture is more complicated. Solanki & Steenbock (1988) predicted, for a cool HSRA-like model (Gingerich et al. 1971), differences of about 0.1 dex between LTE and NLTE iron abundances determined for Fe I lines with low excitation potentials.

For weak iron lines we found that the influence of the multidimensional convection on the abundance determination is about 0.1 dex. A slightly larger value (up to 0.16 dex for A_w) was obtained for the Li I line. Furthermore, we do not confirm the suggestion of Kurucz (1995) that the convection should weaken the lithium lines. Our computations show that the 2-D models produce even stronger Li lines than 1-D homogeneous ones. Note, however, that this result depends upon the spectrum of inhomogeneities in 2-D time-dependent models.

Kurucz (1995) suggested that the multidimensional convection in metal-deficient dwarfs of solar T_{eff} may affect the observed lithium abundances ($\log N(\text{Li}) = 2.1$; Spite & Spite 1982). Many investigators trust that the Spite plateau halo stars have conserved their primordial lithium (Rebolo 1991). So Kurucz's conclusion seems critical for many branches of modern astrophysics. However a few suggestions made by Kurucz should be reconsidered. For example, he used the model granule extended over the whole atmosphere. Due to a higher temperature inside that granule, the ratio $\text{Li II}/\text{Li I}$ in the region of Li I

lines formation region increases. As a result, the lithium abundances, obtained from the Li I line modeling should increase also. From multidimensional computations it is well known that the temperature over a granule region may be cooler as well as hotter than the surrounding matter (at different geometric heights in the atmosphere, see Atroshchenko & Gadun 1994). We note, however, that overshooting convection in halo dwarfs may change their nature with respect to the Sun. Indeed, in halo dwarf atmospheres we can see deeper layers that may have a larger contrast. On the other hand, the radiative cooling of granules in metal-poor atmospheres is more efficient due to the same reason, namely the opacity decrease. To obtain more reliable conclusions the numerical simulation of 2-D and 3-D convection is needed. That work is in progress.

Acknowledgements. Authors thank an anonymous referee for helpful comments. A. Gadun is grateful to European Southern Observatory (Grant A-07-015) and to the Joint Fund of the Government of Ukraine and International Science Foundation (Grant K11100) for the support of this work. We are indebted to R. García López for carefully reading the manuscript.

References

- Atroshchenko I.N., 1993, *Kinemat. i Fiz. Nebesn. Tel* 9, no. 1, 3
 Atroshchenko I.N., Gadun A.S., 1994, *A&A* 291, 635
 Belozerkovskiy O.M., Davidov Yu.M., 1982, *The Method of Large Particles*. Nauka, Moscow
 Blackwell D.E., Booth A.J., Haddock D.J., Petford A.D., Leggett S.K., 1986, *MNRAS* 220, 549
 Blackwell D.E., Ibbetson P.A., Petford A.D., Shallis M.J., 1979, *MNRAS* 186, 633
 Bruls J.H.M.J., Rutten R.J., 1992, *A&A* 265, 257
 Carlsson M., Rutten R.J., Bruls J.H.M.J., Shchukina N.G., 1994, *A&A* 288, 860
 Gadun A.S., 1986, *Simulation of Turbulent Convection in the Solar Envelope*, *Inst. Theor. Phys., Kiev*, preprint no. 86-106P
 Gadun A.S., 1994, *Kinemat. i Fiz. Nebesn. Tel* 10, no. 3, 33
 Gadun A.S., 1995, *Kinemat. i Fiz. Nebesn. Tel* 11, no. 3, 54
 Gadun A.S., 1996, *Kinemat. i Fiz. Nebesn. Tel* 12, no. 4, 19
 Gadun A.S., Pikalov K.N., 1996, *Solar Phys.*, 166, 43
 Gadun A.S., Sheminova V.A., 1988, *SPANSAT: Program for LTE-calculations of Absorption Line Profiles in Stellar Atmospheres*, *Inst. Theor. Phys., Kiev*, preprint no. 88-87P
 Gadun A.S., Vorob'yov Yu.Yu., 1995, *Solar Phys.* 159, 45
 Gingerich O., Noyes R.W., Kalkofen W., Cuny Y., 1971, *Solar Phys.* 18, 347
 Gurtovenko E.A., Kostyk R.I., 1989, *Fraunhofer Spectrum and System of Solar Oscillator Strengths*, *Naukova Dumka, Kiev* (GK89)
 Holweger H., Müller E.A., 1974, *Solar Phys.* 39, 19
 Kurucz R.L., 1979, *ApJSS* 40, no. 1, 1
 Kurucz R.L., 1992, *Rev. Mex. Astron. Astr.* 23, 45
 Kurucz R.L., 1993, *ATLAS9 Stellar Atmosphere Programs and 2 km/s Grid*, CD-ROM 13
 Kurucz R.L., 1995, *Prepr. of Harvard-Smith. Cent. of Asrtrophys.*, no. 4054, 1
 Nordlund Å., 1984, *Modelling of Small-Scale Dynamical Processes: Convection and Wave Generation*. In: Keil S.L. (ed.) *Small-Scale Dynamical Processes in Quiet Stellar Atmospheres*, SPO, Sunspot, p. 181
 Pavlenko Ya.V., 1991, *SvA* 35, no. 2, 212
 Pavlenko Ya.V., 1994, *SvA* 71, no. 4, 600
 Pavlenko Ya.V., 1995, *Mem. It. Astron. Soc.* 62, no. 2, 441
 Pavlenko Ya.V., Rebolo R., Martin E.L., Garcia Lopez R.J., 1995, *A&A* 308, 807.
 Rebolo R., 1991, *Lithium and Berillium in Main-Sequence Stars*. In: Michaud G. and Tutukov A. (eds.) *Proc. IAU Symp. 145, Evolution of Stars: The Photospheric Abundance Connection*, Kluwer, Dordrecht, p. 85
 Smagorinsky J., 1963, *Mon. Weather Rew.* 917, 99
 Solanki S.K., Steenbock W., 1988, *A&A* 189, 243
 Spite F., Spite M., 1982, *A&A* 115, 357
 Steenbock W., Holweger H., 1984, *A&A* 130, 319
 Steffen M., 1989, *Spectroscopic Properties of Solar Granulation Obtained from 2-D Numerical Simulations*. In: Rutten R.J. and Severino G. (eds.) *Solar and Stellar Granulation*, Kluwer, Dordrecht, p. 425
 Steffen M., Gigas D., 1985, *Solar Granulation: Numerical Simulation and Resulting Disc-Center Line Profiles*. In: Schmidt H.U. (ed.) *Theoretical Problems in High Resolution Solar Physics*, MPI, München, p. 95
 Stein R.F., Nordlund Å., 1989, *ApJ* 342, L95
 Thomas R.N., 1957, *ApJ* 125, 260
 Wiese W.L., Smith M.W., Miles B.W., 1966, *NBS Reference data* 1, 4